○ Micro and Nano Systems Letters

LETTER

CrossMark

Folding-paper-based preconcentrator for low dispersion of preconcentration plug

Kyungjae Lee, Yong Kyoung Yoo, Sung Il Han, Junwoo Lee, Dohwan Lee, Cheonjung Kim and Jeong Hoon Lee[*]

Abstract

Ion concentration polarization (ICP) has been widely studied for collecting target analytes as it is a powerful preconcentrator method employed for charged molecules. Although the method is quite robust, simple, cheap, and yields a high preconcentration factor, a major hurdle to be addressed is extracting the preconcentrated samples without dispersing the plug. This study investigates a 3D folding-paper-based ICP preconcentrator for preconcentrated plug extraction without the dispersion effect. The ICP preconcentrator is printed on a cellulose paper with pre-patterned hydrophobic wax. To extract and isolate the preconcentration plug with minimal dispersion, a 3D pop-up structure is fabricated via water drain, and a preconcentration factor of 300-fold for 10 min is achieved. By optimizing factors such as the electric field, water drain, and sample volume, the technique was enhanced by facilitating sample preconcentration and isolation, thereby providing the possibility for extensive applications in analytical devices such as lateral flow assays and FTA[R] cards.

Keywords: Ion concentration polarization (ICP), Preconcentration, Paper, FTA[R] card, Separation, Extraction

Background

Ion concentration polarization (ICP) phenomena, wherein ion concentrations are distributed at the interface between an ion exchange membrane (IEM) and an electrolyte having an electric potential [1], are intensively studied in the field of micro/nanofluidics [2–6]. In general, ICP occurs near an IEM via the permeation of specific charged ions (cation or anion). The ion enrichment and depletion zones are generated in the fluidic channel [1]. Employing micro/nanofluidic networks, the ICP phenomena are frequently utilized to preconcentrate charged sample analytes [3, 7, 8]. Han et al. have investigated ICP preconcentration of various biomolecules in fluidic systems [9–11]. Moreover, desalination of seawater using ICP phenomena has been reported [12, 13].

Although many studies investigated analytical systems for both analytical and point-of-care (POC) applications [14–16], detecting biomolecules at concentrations below the limit of detection (LOD) is still a critical issue for analytical devices. To address this problem, an ICP-based preconcentrator has been developed [17, 18] for enhancing the LOD. In many cases, the preconcentration plug, particularly used for the delivery of preconcentrated samples to external equipment and devices, needs to deliver the samples with minimal dispersion; however, the dispersion of the sample plug is a critical issue [19]. When the electric field is removed, the force balance between external hydraulic force/electric field and depletion force cannot be maintained. Hence, the ICP preconcentration plug is drastically dispersed in the fluidic channel, which severely hampers the use of preconcentration devices with external analytical devices (i.e., mass spectrometry and sensors).

To extract and separate the preconcentration plug, Chen et al. [7] made use of the difference in electrophoretic mobility and a magnetic valve, however, one still needs simple methods without complex additional components. Recently, Kwak and Hong et al. proposed a paper-based ICP preconcentrator to facilitate extraction. Hong et al. developed a continuous-flow preconcentrator with a bifurcation system to collect and separate the samples [19, 20] Recently, we proposed a paper-based preconcentrator, which preconcentrates FITC—albumin with a high preconcentration factor of up to 310-fold

*Correspondence: jhlee@kw.ac.kr
Department of Electrical Engineering, Kwangwoon University, 447-1 Wolgye, Nowon, Seoul 139-701, Korea

Lee *et al. Micro and Nano Syst Lett* (2017) 5:11

Page 2 of 7

for 400 s [3], however, there are limitations in applying the preconcentrator for using external analytical devices because of dispersion of preconcentrated sample plug. In this study, a 3D foldable-paper-based ICP preconcentration system is proposed for obtaining a preconcentration plug with minimal dispersion. By employing the 3D pop-up structure, the preconcentration plug was concentrated and isolated up to 300-fold, which is directly applicable for POC test kits and FTA^R cards.
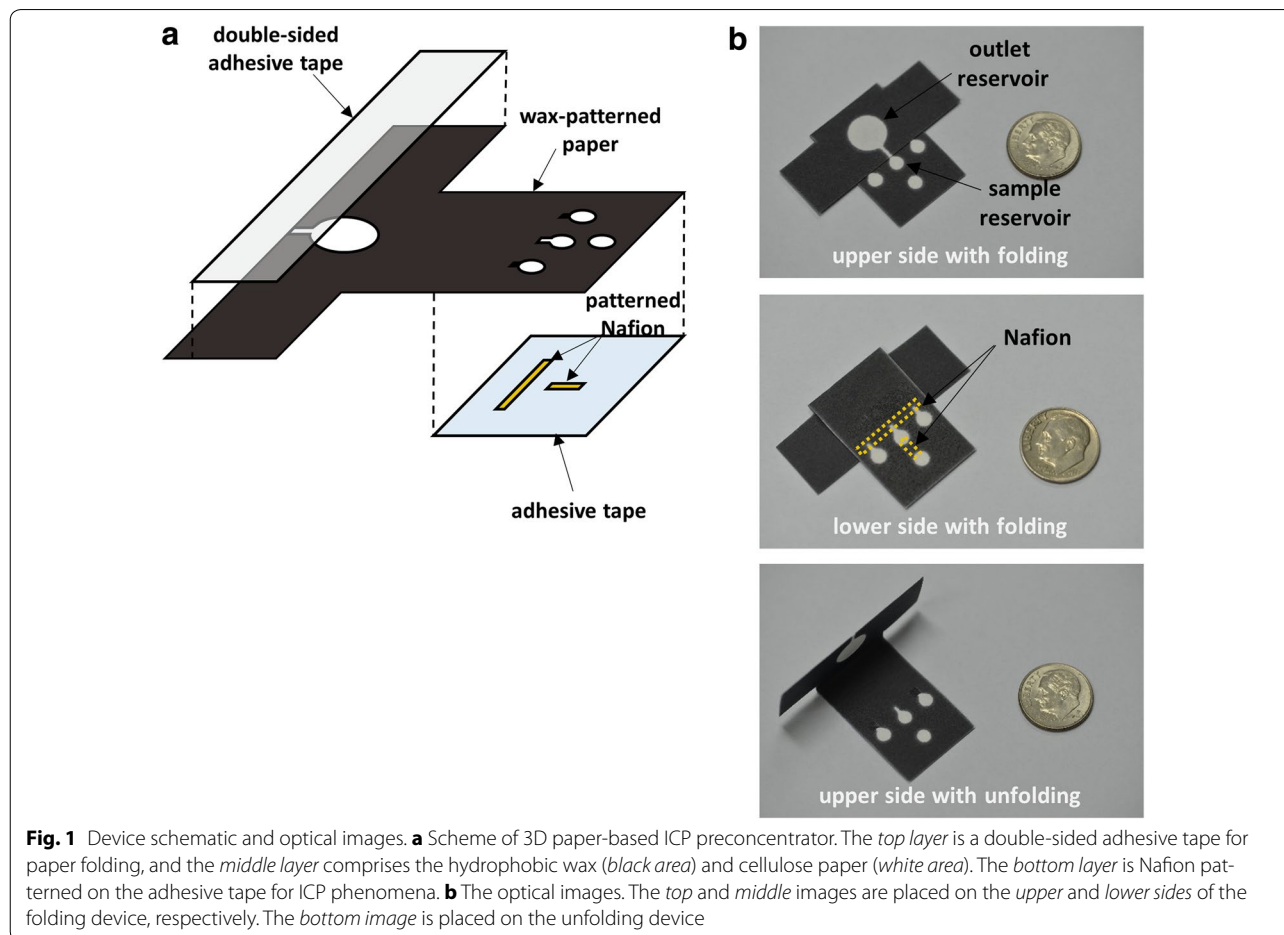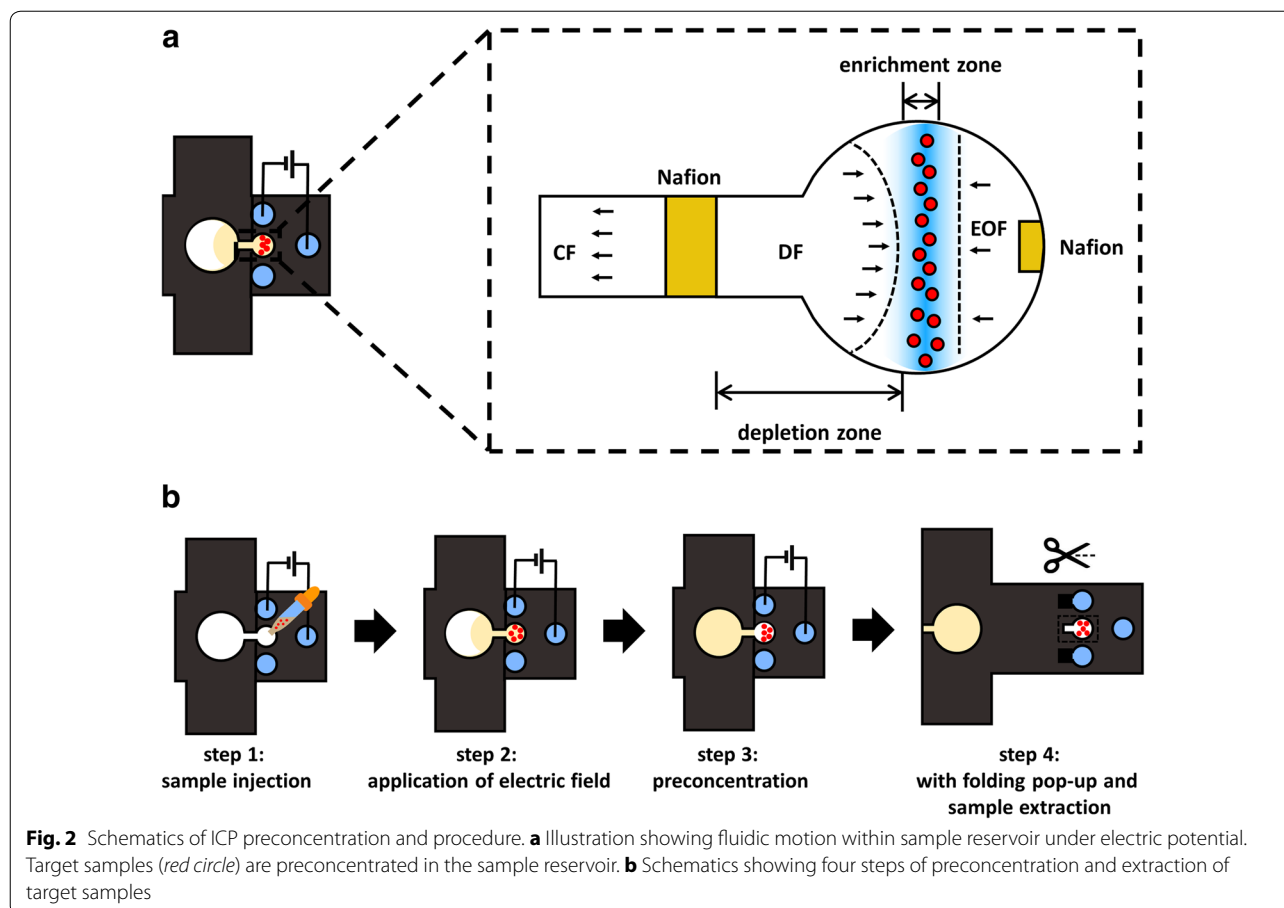
Methods
Device fabrication
As shown in Fig. 1a, b, the 3D folding-paper-based ICP preconcentrator comprises sample and buffer reservoirs, a folding-type outlet reservoir, channels, and Nafion patterns (known as cation exchange membrane). The sample and buffer reservoirs have a diameter of 3 mm, and the outlet reservoirs have diameters of 3, 6 and 9 mm. Each reservoir is connected with a fluidic channel of dimensions 1 × 1.5 mm. The Nafion membranes (1 × 7 and 1 × 14 mm, Sigma-Aldrich, St. Louis, MO) comprising two patterns are immobilized between each

reservoir using one-sided adhesive tape (3 M Scotch™ tape with a width of 18 mm). To apply electric potential, Ag/AgCl electrodes are located on the buffer reservoirs, as shown in Fig. 2a. The preconcentrator was designed using CorelDraw software (Coral Co., Canada), and the patterned hydrophobic wax was printed on a cellulose paper (Whatman chromatography cellulose paper, Grade 1). A commercial wax printer (ColorQube 8870, Xerox) was used for the hydrophobic barrier [21, 22]. To penetrate the wax inside the paper, the wax-printed paper was heated using convection oven at 120 °C for 80 s. To prevent leakage of the samples, the opposite side of the paper is printed and sealed with highly transparent one-sided adhesive tape.

Device operation and preconcentration monitoring
Figure 2b shows the sequential process of the operation principle of the 3D folding-paper-based ICP preconcentrator. First, a sample of 10 μL (NaCl buffer of 1 mM) is loaded onto the buffer reservoirs. An electric potential of 100 V/cm using Ag/AgCl electrodes is applied between the buffer reservoirs via a benchtop
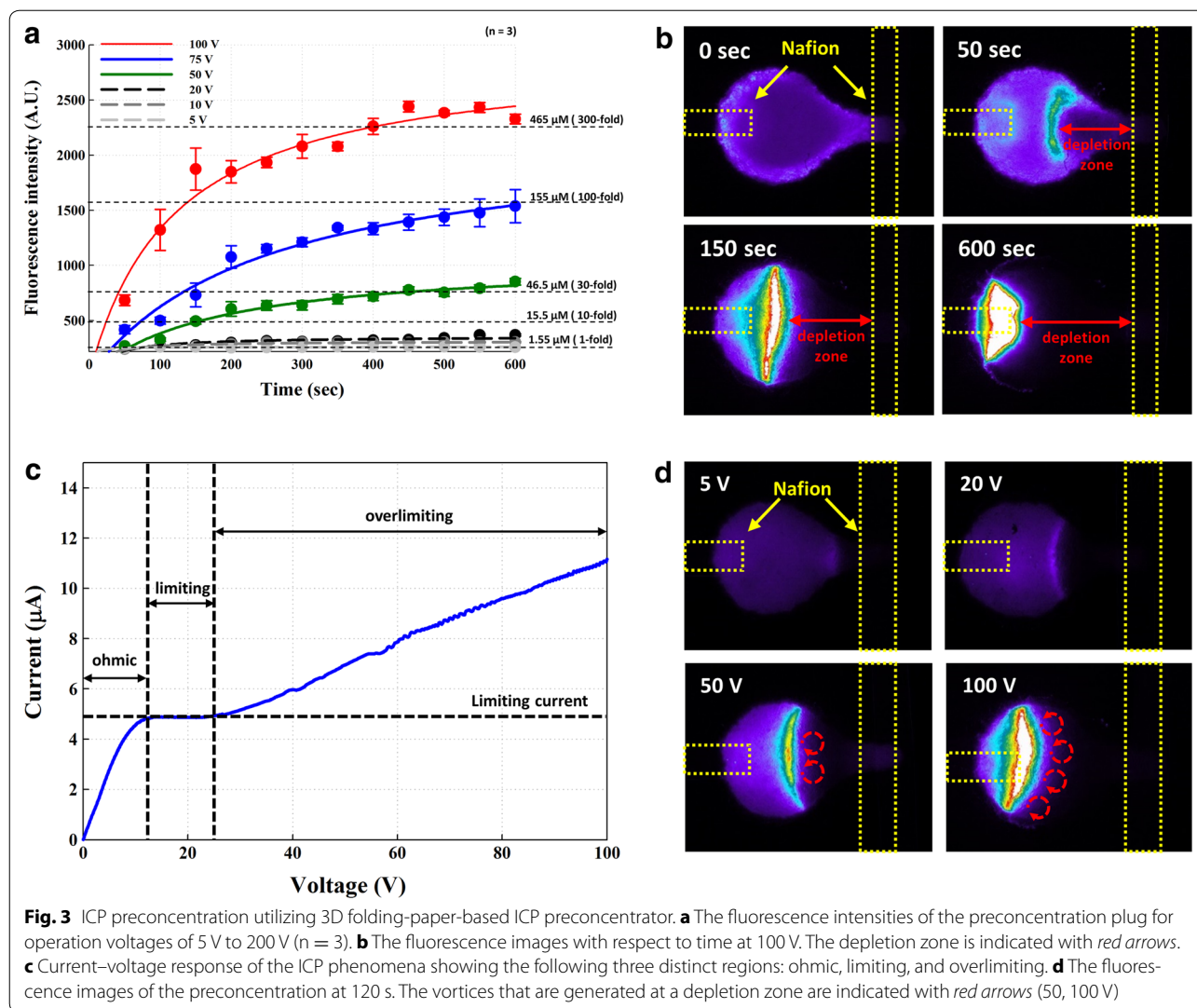

Fig. 1 Device schematic and optical images. **a** Scheme of 3D paper-based ICP preconcentrator. The *top layer* is a double-sided adhesive tape for paper folding, and the *middle layer* comprises the hydrophobic wax (*black area*) and cellulose paper (*white area*). The *bottom layer* is Nafion patterned on the adhesive tape for ICP phenomena. **b** The optical images. The *top* and *middle* images are placed on the *upper* and *lower sides* of the folding device, respectively. The *bottom image* is placed on the unfolding device

Lee *et al. Micro and Nano Syst Lett* (2017) 5:11

Page 3 of 7

Fig. 2 Schematics of ICP preconcentration and procedure. **a** Illustration showing fluidic motion within sample reservoir under electric potential. Target samples (*red circle*) are preconcentrated in the sample reservoir. **b** Schematics showing four steps of preconcentration and extraction of target samples

sourcemeter (Keithley 2410 current–voltage source measurement unit, Keithley Instruments, Inc.). When the electric potential is applied, the sample analytes of volume 10 μL are loaded onto the sample reservoir. They are monitored using an inverted epifluorescence microscope (Olympus, IX-71) and a thermoelectrically cooled charge-coupled device camera (Hamamatsu Co., Japan). After the preconcentration, the outlet reservoir is folded up, and the separated preconcentration plug of the sample reservoir is detached. To monitor the ICP phenomena, fluorescence dyes (Alexa fluor 488, Invitrogen, Carlsbad, CA, USA) and an orange G dye (Sigma-Aldrich, St. Louis, MO) with a buffer solution are utilized. The fluorescence and optical images are analyzed using ImageJ (Wayne Rasband, National Institutes of Health, Bethesda, MD, USA). We carried out all experiments at controlled R.T. and humidity (R.H. = $55 \pm 5\%$) to avoid run-to-run experimental errors.

Results and discussion

ICP phenomena and preconcentration

Figure 2a shows the working principle of the 3D folding-paper-based ICP preconcentrator. The ICP-based

preconcentrator was operated with a DC voltage of 100 V, and the preconcentrated plug with force balance between the driving force of the depletion zone and the capillary force was obtained. Only the buffer solution was freely drained from the sample reservoir by the capillary action, while the charged molecules remained in the sample reservoir because the depletion zone formed in front of the Nafion pattern was blocked. As shown in Fig. 3a, b, the depletion zone is observed near the anodic Nafion side in the sample reservoir, and the preconcentration plug was successfully generated. Figure 3a shows an increase in the fluorescence intensity with preconcentration time. The preconcentration factor at 600 s increased with electric potential as 1-, 2-, 5-, 30-, 100- and 300-fold for 5, 10, 20, 50, 75 and 100 V, respectively. A high preconcentrator factor (300-fold) was achieved with a sample volume of 10 μL. The I–V curve was measured to check ICP phenomenon. Figure 3c and d show the current–voltage response and corresponding fluorescence intensity of the sample reservoir. Previous studies analyzed the current–voltage response with vortices of electroconvection [19, 23]. In the current–voltage response, the following three regions were observed: ohmic, limiting, and overlimiting.

Lee *et al. Micro and Nano Syst Lett* (2017) 5:11

Page 4 of 7

Fig. 3 ICP preconcentration utilizing 3D folding-paper-based ICP preconcentrator. **a** The fluorescence intensities of the preconcentration plug for operation voltages of 5 V to 200 V (n = 3). **b** The fluorescence images with respect to time at 100 V. The depletion zone is indicated with *red arrows*. **c** Current–voltage response of the ICP phenomena showing the following three distinct regions: ohmic, limiting, and overlimiting. **d** The fluorescence images of the preconcentration at 120 s. The vortices that are generated at a depletion zone are indicated with *red arrows* (50, 100 V)

We observed 100 V, the optimal electric potential that we operated for ICP, are in the overlimiting region that generates vortices of electroconvection.

Device optimization

To optimize the preconcentrator, the preconcentrating factor was measured considering both the outlet reservoir diameter and total preconcentration volume. The diameter affects the capillary force, which aids in water draining, thereby maintaining the force balance for stable preconcentration. For optimizing the device, outlet reservoirs with diameters of 1, 3 and 9 mm were employed. Figure 4a shows the preconcentration factors with respect to varying diameters for 100 V. The fluorescence intensity drastically increased for the outlet reservoir (red line) with a diameter of 9 mm. Preconcentration factors of 40-, 80-, and 300-fold were obtained for diameters of 3 mm (green line), 6 mm (blue line), and 9 mm,

respectively. The results show that a diameter of 9 mm is the optimal size for the outlet reservoir. From Darcy's law, the flow rate can be expressed as follows [20, 24, 25]:

$$Q = -\frac{\kappa A}{\mu L}\Delta p, \tag{1}$$

where Q is the volumetric flow rate, κ is the permeability of the paper with respect to the fluid, μ is the viscosity of the fluid, A is the cross-sectional area of the flow, and Δp is the pressure difference along the direction of flow over length L. The volumetric flow rate of the drain water depends on the cross section of the outlet reservoir (diameter).

The total preconcentration volume is one of the essential criteria for the ICP preconcentration. As shown in Fig. 4b, the preconcentration factor was monitored based on the total preconcentration volume. The preconcentration factors of 50-, 90-, and 300-fold are measured for
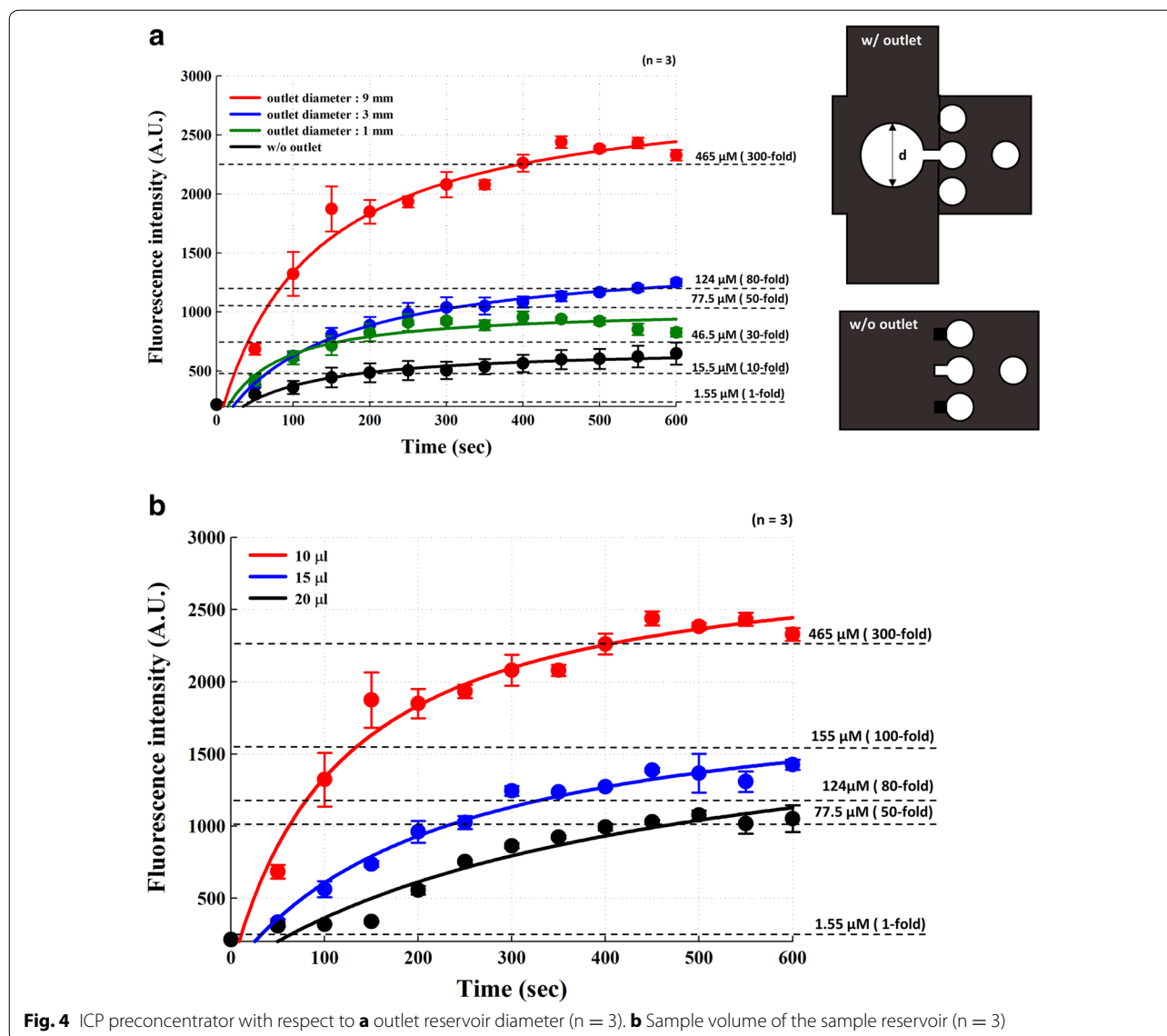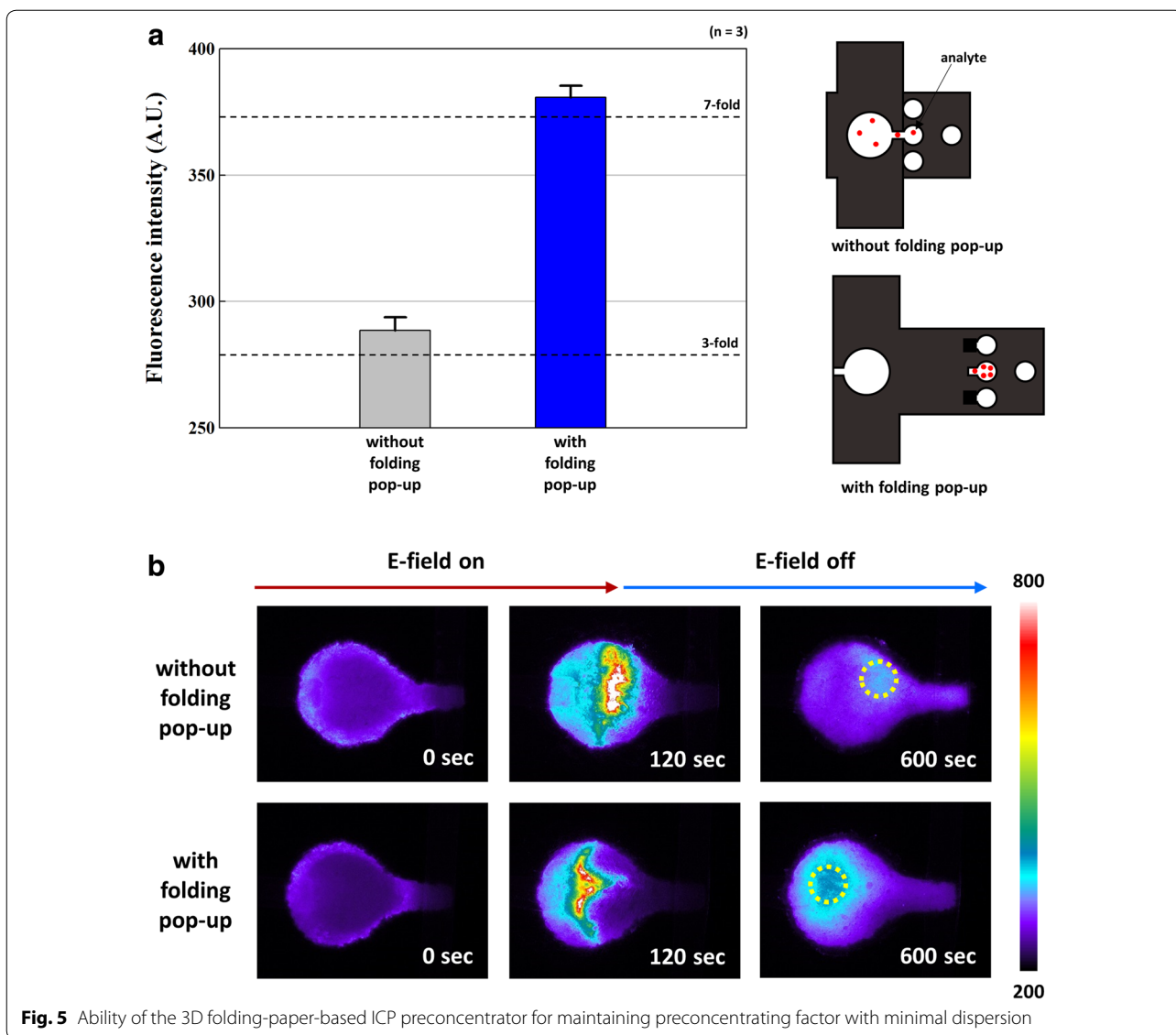
Lee *et al. Micro and Nano Syst Lett* (2017) 5:11

Page 5 of 7

Fig. 4 ICP preconcentrator with respect to **a** outlet reservoir diameter (n = 3). **b** Sample volume of the sample reservoir (n = 3)

volumes of 10 μL (red line), 15 μL (blue line), and 20 μL (black line), respectively. In general, the preconcentrating volume and factor have been considered as a trade-off. If the preconcentrating volume is increased, the preconcentrating factor generally decreases. In Fig. 4b, a higher preconcentrating factor is observed for a total preconcentration volume of 10 μL.

Isolation and extraction of preconcentration plug with folding structure

The ability of the preconcentrator to maintain the preconcentrating factor with minimal dispersion effect was investigated. The following two types of preconcentrators were prepared: with and without folding pop-up structure (Fig. 5a). To check the ability of sust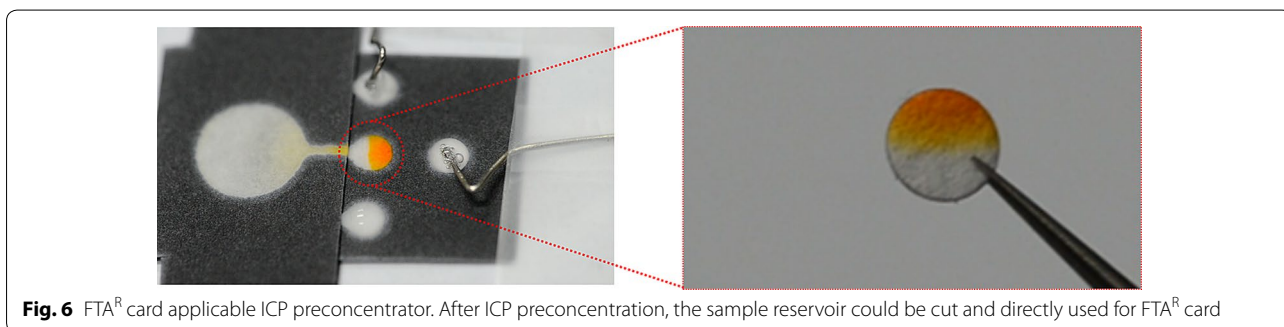aining the preconcentration plug, the preconcentration was performed by draining the buffer solution for 120 s, and subsequently, the electric field was turned off. In turns, we monitored the preconcentration factor with time up to following 8 min. A preconcentration factor of >sevenfolds was observed for the folding pop-up structure, whereas it was ~threefolds (Fig. 5a) for the no-folding pop-up structure. The enhanced fluorescence images were clearly observed with the folding pop-up structure. Figure 5b shows the fluorescence images that are sequentially captured at 0, 120, and 600 s for both with/without folding pop-up structures. The preconcentration was performed for 120 s, and the dispersion of the preconcentration plug was then monitored. Without the folding pop-up structure, the preconcentration plug dispersed toward the outlet reservoir. However, with the folding pop-up structure, the preconcentration plug showed

Lee *et al. Micro and Nano Syst Lett* (2017) 5:11

Page 6 of 7

Fig. 5 Ability of the 3D folding-paper-based ICP preconcentrator for maintaining preconcentrating factor with minimal dispersion

small dispersion, as the capillary forces were eliminated by disconnecting the fluidic channel.

To demonstrate realistic applications, ICP preconcentration of Orange G dye was performed, which facilitated manual inspection (Fig. 6). After the ICP preconcentration for 10 min, with folding pop-up structure, the preconcentration plug with small dispersion was obtained. The preconcentrated sample could be used into two

Fig. 6 FTA^R card applicable ICP preconcentrator. After ICP preconcentration, the sample reservoir could be cut and directly used for FTA^R card

Lee *et al. Micro and Nano Syst Lett* (2017) 5:11

Page 7 of 7

analysis methods. First, following standard FTA extraction protocol, we plan to apply preconcentrated samples for FTA^R cards. Second, we could analyze the preconcentrated sample reservoir using paper-based mass spectrometry [26, 27].

Conclusion

In this study, a 3D folding-paper-based ICP preconcentrator was developed for preconcentrating charged biomolecules with a small dispersion. A preconcentration of 300-fold for a sample volume of 10 μL was obtained. By optimizing the electric field, sample volume, and outlet reservoir size, the 3D folding pop-up paper-based preconcentrator was successfully implemented for extracting the ICP preconcentration plug with low dispersion effects. This technique can be used in applications involving bioassay and environment monitoring (i.e., lateral flow assay, FTA^R card and mass spectrometry).

Abbreviations
ICP: ion concentration polarization; IEM: ion exchange membrane; CF: capillary force; DF: depletion force; EOF: electro-osmotic flow.

Authors' contributions
KJL helped design, fabricate, and test the device and drafted the manuscript. YKY and SIH reviewed the test methods and results. JL, DL, and CK surveyed the literature on ion concentration polarization. JHL reviewed all the test methods and results and finalized the drafted manuscript. All authors read and approved the final manuscript.

Competing interests
The authors declare that they have no competing interests.

References
1. Kim SJ, Song Y-A, Han J (2010) Nanofluidic concentration devices for biomolecules utilizing ion concentration polarization: theory, fabrication, and applications. Chem Soc Rev 39:912–922. doi:10.1039/b822556g
2. Phan DT, Shaegh SAM, Yang C, Nguyen NT (2016) Sample concentration in a microfluidic paper-based analytical device using ion concentration polarization. Sensors Actuators, B Chem 222:735–740. doi:10.1016/j.snb.2015.08.127
3. Il Han S, Hwang KS, Kwak R, Lee J (2016) Microfluidic paper-based biomolecule preconcentrator based on ion concentration polarization. Lab Chip 16:2016. doi:10.1039/C6LC00499G
4. Yeh L, Zhang M, Qian S et al (2012) Ion concentration polarization in polyelectrolyte-modified nanopores. J Phys Chem 116:8672–8677
5. Gong MM, Nosrati R, San Gabriel MC et al (2015) Direct DNA analysis with paper-based ion concentration polarization. J Am Chem Soc 137:13913–13919. doi:10.1021/jacs.5b08523
6. Kim B, Kwak R, Kwon HJ et al (2016) Purification of high salinity brine by multi-stage ion concentration polarization desalination. Sci Rep 6:31850. doi:10.1038/srep31850
7. Chen YY, Chiu PH, Weng CH, Yang RJ (2016) Preconcentration of diluted mixed-species samples following separation and collection in a micro-nanofluidic device. Biomicrofluidics. doi:10.1063/1.4942037
8. Choi D, Choi A, Kim DS (2015) A capillary-based preconcentration device by using ion concentration polarization through cation permselective membrane coating. Int J Precis Eng Manuf 16:1467–1471. doi:10.1007/s12541-015-0194-y
9. Jeong HL, Chung S, Sung JK, Han J (2007) Poly(dimethylsiloxane)-based protein preconcentration using a nanogap generated by junction gap breakdown. Anal Chem 79:6868–6873. doi:10.1021/ac071162h
10. Lee JH, Song Y-A, Han J (2008) Multiplexed proteomic sample preconcentration device using surface-patterned ion-selective membrane. Lab Chip 8:596–601. doi:10.1039/b717900f
11. Lee JH, Song YA, Tannenbaum SR, Han J (2008) Increase of reaction rate and sensitivity of low-abundance enzyme assay using micro/nanofluidic preconcentration chip. Anal Chem 80:3198–3204. doi:10.1021/ac800362e
12. Oh Y, Lee H, Son SY et al (2016) Capillarity ion concentration polarization for spontaneous biomolecular preconcentration mechanism. Biomicrofluidics 10:1–9. doi:10.1063/1.4939434
13. Kim SJ, Ko SH, Kang KH, Han J (2010) Direct seawater desalination by ion concentration polarization. Nat Nanotechnol 5:297–301. doi:10.1038/nnano.2010.34
14. Kwak R, Kim SJ, Han J (2011) Continuous-flow biomolecule and cell concentrator by ion concentration polarization. Anal Chem 83:7348–7355. doi:10.1021/ac2012619
15. Engler AJ, Sen S, Sweeney HL, Discher DE (2006) Matrix elasticity directs stem cell lineage specification. Cell 126:677–689. doi:10.1016/j.cell.2006.06.044
16. Sista R, Hua ZS, Thwar P et al (2008) Development of a digital microfluidic platform for point of care testing. Lab Chip 8:2091–2104. doi:10.1039/b814922d
17. Yetisen AK, Akram MS, Lowe CR (2013) Paper-based microfluidic point-of-care diagnostic devices. Lab Chip 13:2210–2251. doi:10.1039/c3lc50169h
18. Hsieh K, Ferguson BS, Eisenstein M et al (2015) Integrated electrochemical microsystems for genetic detection of pathogens at the point of care. Acc Chem Res 48:911–920. doi:10.1021/ar500456w
19. Kwak R, Kang JY, Kim TS (2016) Spatiotemporally defining biomolecule preconcentration by merging ion concentration polarization. Anal Chem 88:988–996. doi:10.1021/acs.analchem.5b03855
20. Hong S, Kwak R, Kim W (2016) Paper-based flow fractionation system applicable to preconcentration and field-flow separation. Anal Chem 88:1682–1687. doi:10.1021/acs.analchem.5b03682
21. Martinez AW, Phillips ST, Carrilho E et al (2008) Simple telemedicine for developing regions: camera phones and paper-based microfluidic devices for real-time, off-site diagnosis. Anal Chem 80:3699–3707. doi:10.1021/ac800112r
22. Martinez AW, Phillips ST, Nie Z et al (2010) Programmable diagnostic devices made from paper and tape. Lab Chip 10:2499. doi:10.1039/c0lc00021c
23. Minerick AR, Ostafin AE, Chang HC (2002) Electrokinetic transport of red blood cells in microcapillaries. Electrophoresis 23:2165–2173. doi:10.1002/1522-2683(200207)23:14<2165::AID-ELPS2165>3.0.CO;2-#
24. Fu E, Ramsey SA, Kauffman P et al (2011) Transport in two-dimensional paper networks. Microfluid Nanofluidics 10:29–35. doi:10.1007/s10404-010-0643-y
25. Masoodi R, Pillai KM (2010) Darcy's law-based model for wicking in paper-like swelling porous media. AIChE J 56:2257–2267. doi:10.1002/aic.12163
26. Wang H, Liu J, Graham Cooks R, Ouyang Z (2010) Paper spray for direct analysis of complex mixtures using mass spectrometry. Angew Chemie-Int Ed 49:877–880. doi:10.1002/anie.200906314
27. Liu W, Mao S, Wu J, Lin J-M (2013) Development and applications of paper-based electrospray ionization-mass spectrometry for monitoring of sequentially generated droplets. Analyst 138:2163–2170. doi:10.1039/c3an36404f